Journal of Earth and Atmospheric Research

SEASONAL WAVE CLIMATE ON THE NIGER DELTA SHORELINE: TEMPORAL VARIABILITY AND IMPLICATION

*[1]Dada O. A., [1]R. B. Adesina., and [1]Agbaje A. O.

[1]Department of Marine Science and Technology, Federal University of Technology, Akure, Nigeria

Article History
Received: April 3, 2018
Revised: May 29, 2018
Accepted: June 20, 2018

Keywords:
Coastline change, coastal processes, seasonal change, hydrodynamic factors, Gulf of Guinea

ABSTRACT

The shoreline is an interface between land and water where continuous changes occur at diverse spatial and temporal scales. Thus, seasonal shoreline changes constitute an important aspect of temporal variability of the coastal environment. In this study, we investigated seasonal wind and wave climate and their implications on the Niger Delta (ND) shoreline in the Gulf of Guinea of the North Atlantic. We extracted shorelines for a period of 6 years (2008-2013) from remote sensing data and coupled them with wind and wave data for the same period. The results showed that shoreline advance coincides with low-energetic conditions which characterized winter months (wet/rainy season), while accentuated shoreline retreat coincides with high-energetic conditions which characterized summer months (dry season). The studied winds (up to 5 m/s in winter, but can reach up to 10 m/s in summer) and waves (wave period and wave height up to 12 s, and <1.9 m in winter, respectively, but can be >12 s and up to 3.2 m in summer) follow the same patterns, as they are characterized by calm and low-energetic conditions in winter months and high-energy conditions in summer months. The same as offshore winds that blow primarily and predominantly towards the coast in the NNE direction from the SSW quadrant, waves also approach the coast primarily from the SW, irrespective of the season. Shoreline variations strongly correlate with the wind speed (R^2 = 0.903), and the significant wave height (R2 = 0.962), which strongly suggest that seasonal forces of wind and waves influence shoreline dynamics of the study area. However, other environmental factors not mentioned in the study may also contribute to these changes.

1.0 INTRODUCTION

Shoreline or coastline is the line that coincides with the physical interface between land and water (Feng, et al., 2014; Gokceoglu et al 2014; Louati et al., 2014), and is one of the rapidly changing coastal geomorphic (Louati et al., 2014). These rapidly changing shorelines pose a serious problem to most deltas on earth (Louati et al., 2014). Thus, accurate and timely information on shoreline dynamics in these sensitive and vulnerable areas is needed. The Niger Delta (ND) in the Gulf of Guinea of North Atlantic is one of the most important deltas in the world, but the least studied; more so, studies on its shoreline dynamics are scarce due to the dearth of data (Kuenzer et al., 2014). However, with the advent of remote sensing, (a real-time, faster, accurate, low cost and all-weather technology), coupled with geographic information system (GIS), it is easier to obtain timely information on the interactions between land-water interface (Feng, et al., 2014; Cui and Li, 2011; Durduran, 2010). Its multispectral nature and repetitive coverage makes it the most useful for mapping and updating the shoreline dynamics periodically cost-effectively and accurately (Louati et al., 2014)

.

At the same time, understanding the impacts of variations of wave height and wave direction, as well as the timescales of these changes, is also crucial in studying and predicting future shoreline position (Splinter et al., 2012); for a strong correlation exist between seasonal shoreline changes and variations in wave height (e.g., Dada et al., 2016a; Davidson et al., 2010)). Sensuo stricto, larger waves, and more energetic conditions during the winter months are responsible for beach recession, whereas calmer and low-energetic conditions enhance shoreline progradation. Moreover, short-term, seasonal variability in wave climate is the key driver of interannual shoreline variability (Splinter et al., 2012) and is, therefore, an important parameter that needs to be considered. The aim of this paper is to determine the relationship between variations in the wind and wave climate to the changing patterns of seasonal and interannual shorelines in the arcuate sector of the Niger Delta (ND) in the Gulf of Guinea of the North Atlantic.

1.1. THE STUDY AREA

The arcuate sector of the ND (Fig. 1) is located in the southern part of Nigeria along the Gulf of Guinea coast of the North Atlantic Ocean; from the west of Ramos River mouth for a distance of about 284 km to the east of Sombreiro River mouth. It is flanked by the Western and Eastern ND and has about 14 major river mouths/ tidal inlets that intersect the coast, breaking it up into a series of barrier islands (Figure 1; Dada et al., 2016 a, b). It is one of the world's largest arcuate fan-shaped river deltas. The study area accounts for a large expanse of the Nigerian coastline, spreading over a number of ecological zones, sandy coastal ridge barriers, brackish or saline mangroves, meandering creeks, freshwater permanent and seasonal swamp and lowland forests. River Niger, the 3rd largest river in Africa and 9th in the world, drains a large part of West Africa, and discharges its waters, sediments and other loads, through Ramos and Nun rivers in the arcuate sector of the ND before it finally enters into the Atlantic Ocean (Figure 1; Dada et al., 2016a; Abam, 2001). The ND coast is characterized by two dominant seasons: the wet (rainy) season referred to in this study as winter months, and dry season referred to in this study as summer months. The summer (rainy/wet) season spans for a period of eight (8) months, which begins in March and ends in October while the winter (dry) season lasts for four (4) months, from November till February of the following year (Dada et al., 2016a; Adejuwon, 2012). Two air streams affect the weather over the coast of the ND. These are the southwest and northeast monsoons, which represent a large scale cross-equatorial flow of air from South Atlantic Ocean, in summer, and the cool, dry and dusty northeast trade from the Sahara anticyclone, in winter, respectively (Olaniyan and Afiesimama, 2003). The winds associated with southwest monsoon are the southwesterly winds, which are characterized by long-shore currents. However, the type of air

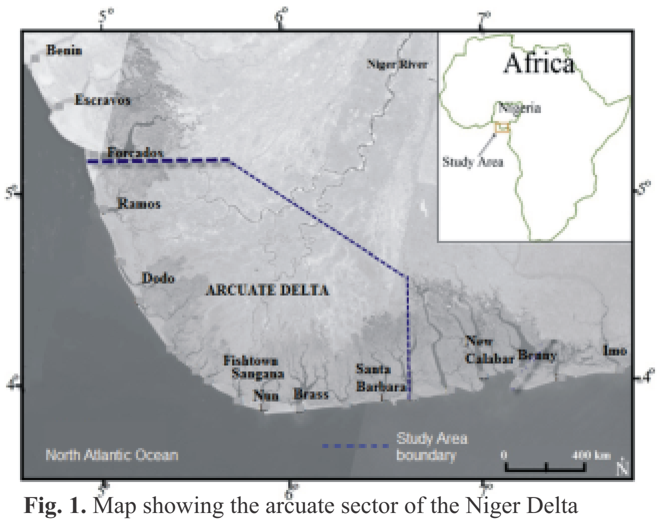

Fig. 1. Map showing the arcuate sector of the Niger Delta in the Gulf of Guinea.

stream that affects the ND coast depends on the position of the Inter-Tropical Discontinuity (ITD) over the country on a regional scale, and globally by the effect of the Walker circulation (Olaniyan and Afiesimama, 2003).

2.0 METHODOLOGY

2.1. SHORELINE CHANGE

2.1.1. DATA ACQUISITION AND PROCESSING

The shoreline positions along the ND during the period from 2008 to 2013 were extracted from Landsat Thematic Mapper at 30 m resolution. The Thematic Mapper images for 30th December, 2008; 4th March, 2009; May 26th 2010; 20th December, 2010, 26th March, 2011; 29th April, 2012; 25th December, 2012; 10th January, 2013 and 20th December, 2013 were acquired in GeoTiff format from the USGS archive (http://glovis.usgs.gov/). The images have 30 m resolution, with each pixel being 30 m by 30 m. Of the bands, Band 5 was used, because it exhibits a strong contrast between land and water features. The high water line (HWL) position, which is recognized as the landward limit of wave run-up at the time of local high tide, was used as a proxy to define shoreline positions on the images (Thieler et al., 2013). As suggested by Thieler et al. (2013), HWL delineation was carried out using the following as proxies : (i) the earlier high tide line seaward of the storm debris wrack line, as shown by changes in tonal between wet and dry beach material, a vegetation line; (ii) the high-tide wrack line, created when the high tide deposits seaweed and debris on the upper beach; and (iii) the maximum wave run-up limit at or near high tide indicated by the interface between the land and water. The area considered for the present study was along the 267,000 km of the arcuate flank of the Niger Delta, from the west Ramos river (5.23o N, 5.35o E) mouth to the west of San Bartholomew river mouth (4.34o N, 6.71o E).

All images were referenced to the World Geodetic System (WGS84) datum and projected using the Universal Transverse Mercator system (zone UTM 31 North). The discrete shoreline was extracted, aggregated into one GIS shapefile and exported into a personal geodatabase file, using ArcGIS software. The rate of change statistics for aggregated shorelines was computed, using DSAS 4.2 software (Thieler et al., 2009). In the DSAS 4.2 software, each shoreline segment had a date, uncertainty, length, shape, and object ID field. A second input was a set of shore-perpendicular transects extending from an off-shore baseline, landward to 2.5 km. Transect spacing for this analysis was set at 500 meters. The distance between shorelines and shoreline displacement was measured from a baseline, with seaward shoreline movements represented by positive (+) numbers and landward movements represented by negative (-) numbers. Transects were manually edited to prevent calculation of rates at the river mouths/inlets, and areas where less than ten shorelines intersected. All results used in this study were determined at a 99.7% confidence interval with a +/- 0.03 m spatial error. As suggested by Dada et al. (2015, 2016a), uncertainty in this study was categorized into proximity error and measurement uncertainty, and the maximum annualized error calculated for the Niger Delta, Gulf of Guinea was 1.05 meters/year.

2.1.2. CALCULATING NET SHORELINE CHANGE

The DSAS Software extension was used to compare shoreline positions and calculate the net shoreline movement (NSM, in meters) along the beach at designated transect locations at set intervals from 2008-2013. NSM represents the total distance between the oldest and youngest shorelines (Theiler et al., 2009).

2.2. WAVE AND WIND DATA

Due to unavailability of buoy data for wave and wind measurements in the study area, modelled-derived NWW3 wave and satellite-derived wind data were used in the present study. NOAA Wavewatch3 (NWW3) is a third-generation spectral model for wind wave development and propagation that solves the action balance equation for the evolution of the wave spectrum under wind forcing, archived at http://polar.ncep.noaa.gov/waves. The model is operational on latitude/longitude (1° x 1.25°) grid, and significant wave height, period and direction have been archived at 3-hourly intervals since 1997. We extracted significant wave height, period and direction for the Niger Delta region for the period January 2008 to December 2013 from the archived NWW3 data. In the present study, e wave direction was defined based on the meteorological convention (i.e. as the direction wave was travelling/ coming from).

The wind data for this study was obtained from the QuikSCAT (archived at ftp://podaac-ftp.jpl.nasa.gov/allData/quikscat/L3/jpl/v2/hdf/). The data have meridional and zonal components of wind values, measured twice a day in 0.25o x 0.25o global coverage grid, in an ascending and descending pass. The wind directions were defined using the oceanographic convention that 0o indicated that the winds were blowing towards the north and 90o towards the east. The simple statistical analysis was carried out on wind speed and direction, significant wave height, direction and period to understand their seasonal variability. The wind and wave data were extracted at the position, geographically separated by 25-80 km away from the coast at a depth not greater than 100 m.

Regarding data reliability for the study, unfortunately, buoy data were not available for wave and wind measurements within the range of the Gulf of Guinea and those close to this region were near the coast where matching QuikSCAT winds and NWW3 wave data were unavailable. This issue also had been noted in previous studies (e.g., Pickett et al. 2003; Tang et al. 2004). Hence it was not possible to compare wind and wave data from QuikSCAT and NWW3, respectively, directly with buoy data from the study area. However, it has been well-proven that QuikSCAT is a useful tool to study the wind-induced phenomena in the open ocean and near the coast. Several studies have compared QuikSCAT wind data to buoys all over the global ocean; for instance, over the global ocean (Wallcraft et al., 2009), the Indian Ocean (Satheesan et al. 2007), the Mediterranean Sea (Accadia et al. 2007; Bentamy et al. 2007; Ruti et al., 2008; Pensieri et al. 2010), the Galician coast (Alvarez et al., 2006; 2008), the northwestern Iberian Peninsula (Penabad et al., 2008) the U.S. northwestern coast (Tang et al. 2004) and the U.S. western coast (Chelton and Freilich 2005; Pickett et al. 2003). All these studies found that QuikSCAT wind data tend to have similar accuracy as buoy data in the open ocean. As shown in Table 1, QuikSCAT winds outperformed other satellite-based and numerically wave produced (NWP) products such as Navy Operational Global Atmospheric Prediction System (NOGAPS), European Centre for Medium-Range Weather Forecasts (ERA-40) and National Center for Environmental Protection (NCEP) over the global ocean. For the wave climate analysis, the

NWW3 datasets have been extensively used in previous studies to examine interannual wave climate variability at the Brazilian offshore (e.g., Pianca et al., 2010), along the west of Iberia (e.g., Rusu et al., 2008), coast of Portugal (e.g., Sebastio et al., 2000). As shown in Table 2, the NWW3 waves outperformed Altimetry, ERA-40 and CERA-40 wave in the Southern Hemisphere (Australia). Thus, we believe that the high skill level achieved in general with these data in the previous studies is applicable here.

Table 1. Comparisons of monthly mean 10 m wind speeds from buoys, satellites and NWP products over the global ocean (modified after Wallcraft et al., 2009).

	Bias (m/s)	RMSE (m/s)	δ Buoy (m/s)	δ Products (m/s)	R	SS
QSCAT v. Buoy	0.33	0.73	1.72	1.69	0.92	0.8
SSM/I v. Buoy	0.33	0.81	1.72	1.61	0.9	0.78
NOGAPS v. Buoy	-0.72	1.08	1.72	1.49	0.88	0.6
ERA-40 v. Buoy	-0.61	1.07	1.72	1.77	0.86	0.61
NCEP v. Buoy	0.5	0.97	1.72	1.77	0.86	0.7

Note: Statistics are based on 1281 monthly mean winds obtained from all 137 buoys (i.e. NDBC, TAO, PIRATA). QSCAT = Sea winds instruments on the Quick Scatterometer (0.250^0 x 0.250^0); SSM/I = Special Sensor Microwave/Imager (0.250^0 x 0.250^0); NOGAS = Navy Operational Global Atmospheric Prediction System (1.000^0 x 1.000^0); ERA-40 = European Centre for Medium Range Weather Forecasts ($.250^0$ x 1.250^0); NCEP = National Center for Environmental Protection (1.875^0 x 1.875^0). SS = non-dimension skill score, which is fraction of variance explained by any given wind product minus two dimensionless bias; δ Buoy = standard deviation of buoy winds; δ Products = standard deviation of winds from varieties of products i.e. QSCAT, SSM/I, NOGAS, ERA-40 and NCEP.

Table 2. Comparisons of wave heights from buoys, NWW3, Altimeter, ERA-40 and CERA-40 in the Southern Hemisphere (Australia) (Modified after Hemer et al., 2007)

	R	RMSE (m)
NWW3 v. Buoy	0.86	0.63
ALT v. Buoy	0.79	0.75
ERA-40 v. Buoy	0.78	0.59
CERA-40 v. Buoy	0.79	0.58

3. RESULTS

3.1. SEASONAL SHORELINE CHANGE

The seasonal shoreline positions are highly varied between 2008 and 2013 in the study area (Fig. 2). Nevertheless, the dominant shoreline change seasonal pattern showed shoreline advance in winter (dry season) and retreat during summer (wet season) (Fig. 2a, b). Generally, the net shoreline positions during summer months were negative, with mean shoreline change ranging from -6.82 m to -22.38 m (Fig. 2b), while net shoreline changes in winter months were predominantly positive, with mean shoreline change ranging between 9.64 m and 20.48 m (Fig. 2b). As shown in Figure 2, the summer of 2011 and 2012 had the highest shoreline retreat up to -22.38 m (in 2011).

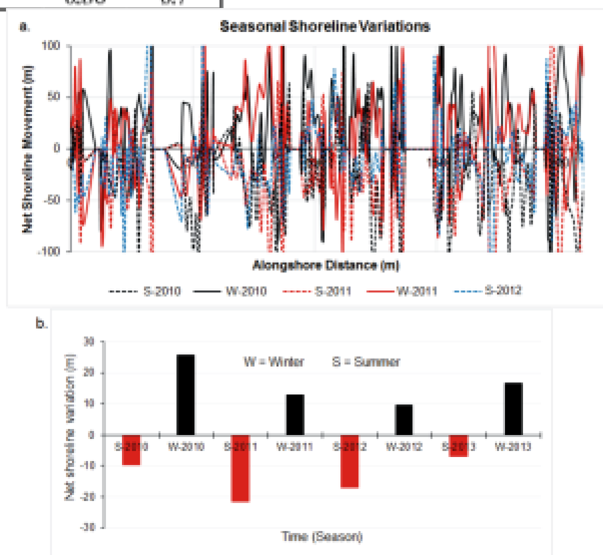

Figure 2. Shoreline change for the arcuate sector of the ND coast, showing (a) 2012 seasonal shoreline variations (2010 to 2012); (b) temporal shoreline variations (2010 to 2013). Note that seaward movements of the shoreline (advance) are identified by positive values and landward movements (retreat) by negative values.

3.2. WIND DATA ANALYSIS

Figure 3 illustrates the offshore wind conditions in the study area during the studied period. Wind speed range between 3 m/s and 5 m/s was most frequent during winter months and doubled in summer months to 8 m/s. High-energy events occurred mainly in the summer months of June, July, August and September (Fig. 3a-c). Maximum offshore wind speed was above 9 m/s during the summer months of July, August and September of 2011, 2012 and 2013 (Fig. 3a-c). The winds were primarily stronger at Sangana-Nun-Brass (as high as 9.6 m/s) and secondarily at the Santa Barbara (up to 8.6 m/s) than any other part of the study area all year round. Also, two minima occurred during the months of April/May and December/January, which represented pre-summer season and peak of the winter season, respectively.

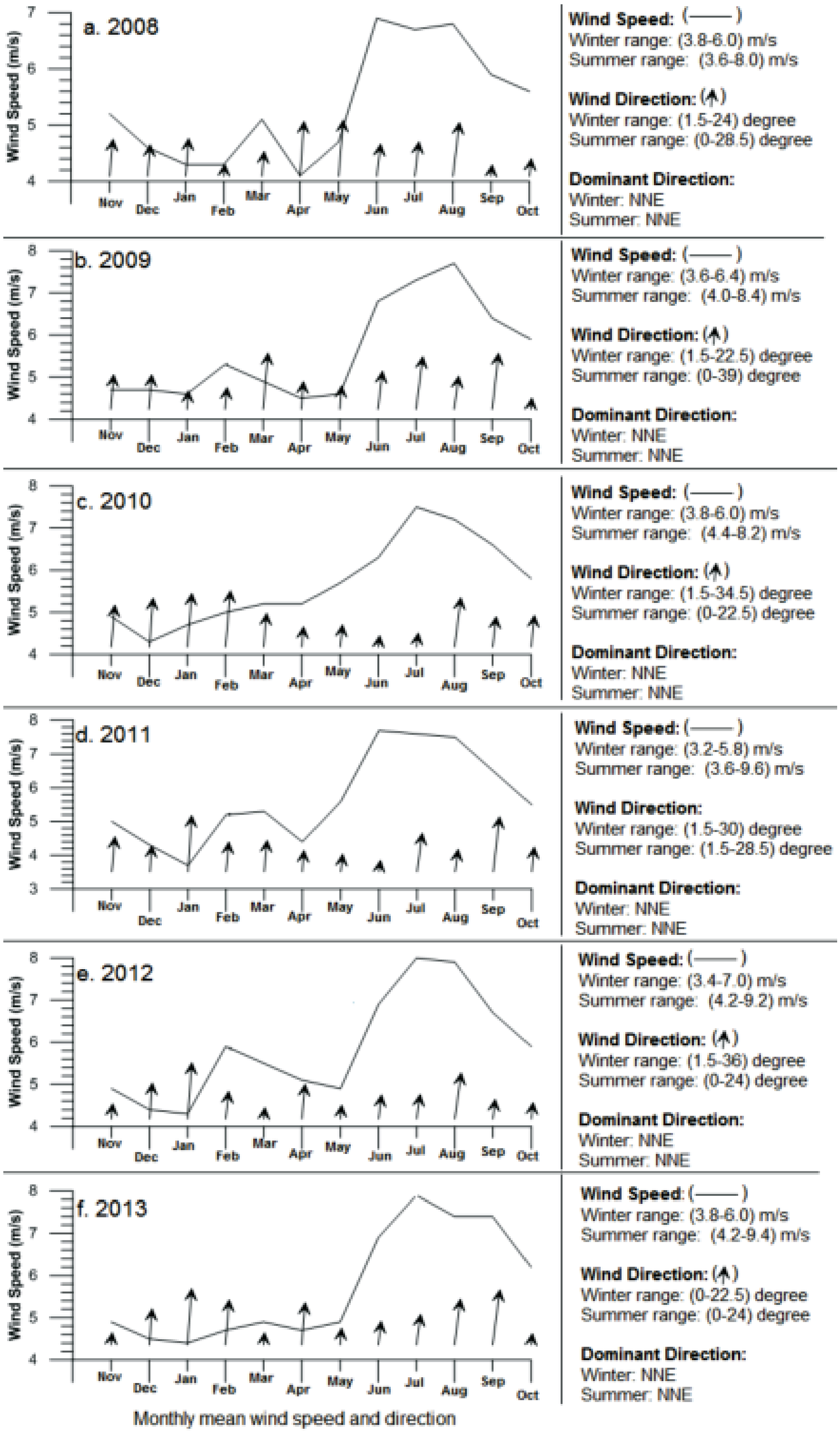

Figure 3. (a-f) Temporal variation of monthly mean offshore wind speed and direction from 2008-2013. Generally, the intensity of wind speeds is higher during the summer months (wet season) of June to October. Note that wind directions are given in degrees and are defined using the oceanographic convention that 0^0 indicates that the winds are blowing towards the north and 90^0 towards the east. In this case, winds blow predominantly from SSW to NNE.

3.3. WAVE DATA ANALYSIS

Figures 4 and 5 illustrate the offshore wave conditions between 2008 and 2013. As observed, the wave conditions in this region reflected seasonal trends of high and low energy. First, calm and low incident wave conditions characterized the winter (dry season). Second, high-energy storm events dominated the summer period. The wave directions ranged from 180^0 and 226.4^0 (predominantly from SW and secondarily from S direction) both in summer and winters months. But waves were frequently from the SW direction at all seasons (Figs 4 and 5c). Wave periods of 12 s were most frequent during winter, whereas they were more than 12 s in summer, and those less than 12 s were less frequent (Fig. 4b). As shown in Figure 4 c-e, wave heights higher than 1.9 m were not common during winter but were up to 2.8 m in summer months. During the studied period, high-energy events occurred mainly in the summer months of June, July and August, and secondarily in March, April, May, September, and October. For instance, maximum offshore wave height reached 3.2 m during the summer month of July and August of 2011 and 2012 (Fig. 4 c-e). Wave heights were observed to be primarily larger between Sangana and Nun (as high as 3.1 m) and secondarily between St Nicholas and Santa Barbara (as high as 2.8 m) than any other part of the study area.

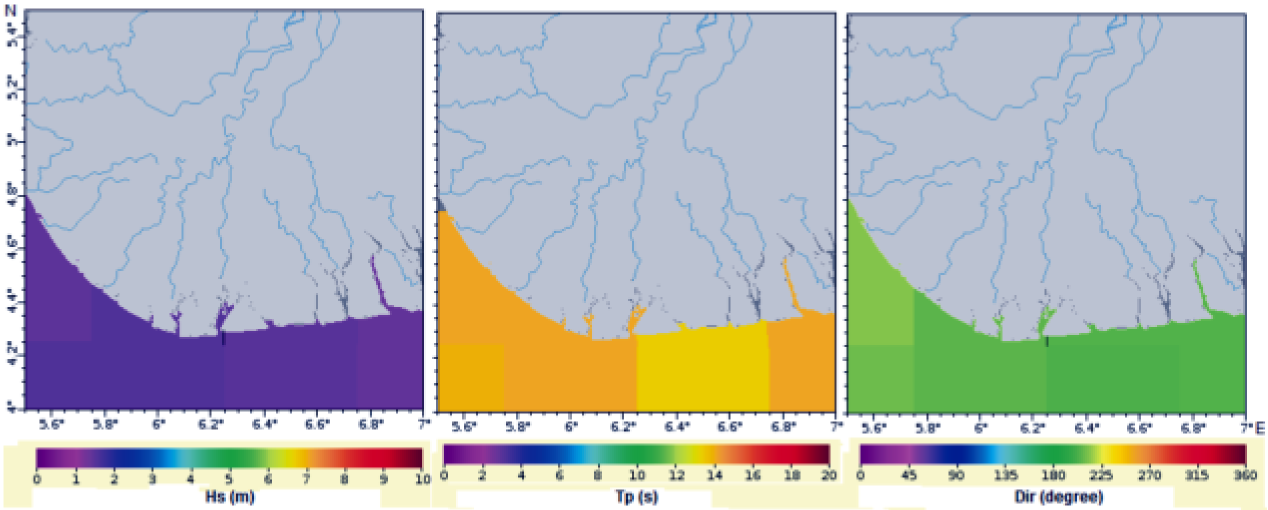

Fig 4. Spatial distribution of annual wave parameters (Hs, Tp and Dir) along the Niger Delta coast. Note that Hs = significant wave height (m), Tp = wave period (s) and Dir = wave direction (degree).

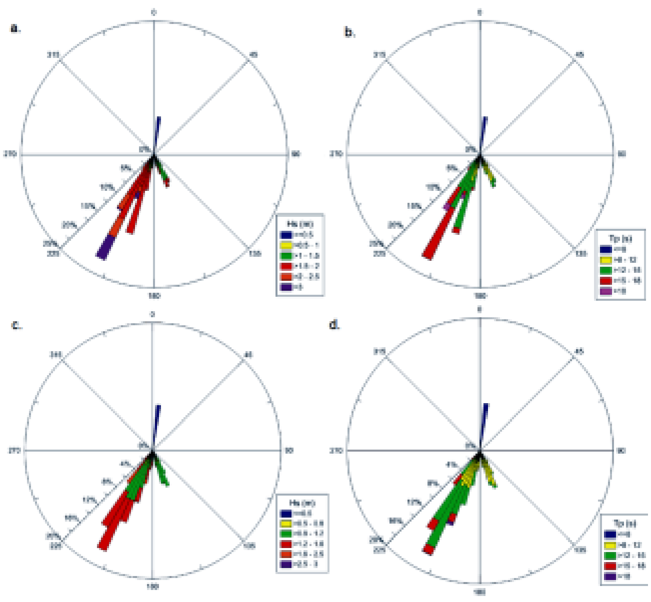

Figure 5. (a.) Typical Seasonal offshore wave climate during (a-b) Summer (rainy season) months of June, July, August and September; (c-d) Winter (dry season) months of November, December, January and February. Note that Hs = significant wave height (m), Tp = wave period (s) and Dir = wave direction (degree).

4.0 DISCUSSION

In this study, we investigated the interaction of shoreline variation with winds and wave variability at seasonal scale in the Niger Delta. We used shoreline data extracted from remote sensing data (Landsat images) for the period of 6 years (between 2008 and 2013) combined with wind and wave data for the same period. The seasonal shoreline variation of the arcuate sector of the ND coast have been analyzed and shown in Figs 2. Likewise, wind and wave analyses results are shown in Figs 3 and 4, respectively.

4.1.1 SEASONAL SHORELINE VARIATIONS

Generally, shoreline advances seaward in winter months because of the fair weather conditions prevailing during this period (Fig. 2). However, this accretion configuration, which is synonymous with the winter months (dry season) between November and February of the following year, is altered during high-energy conditions, which usually prevail during the summer months (wet season), between March and October, to an erosion configuration. According to Joevivek and Chandrasekar (2014), the process of seasonal wave action is cyclic, and it shifts sand materials from berm to nearshore and back again to berm. The variation in the berm and beach slope indicates that excess of wave energy emanating during summer months removes sands from the berm crest offshore. Also, during the high-energy conditions, seaward flowing bottom currents remove sediments from the beach face and move it seaward. At the same time, surging waves create a series of abandoned berms in the backshore region. The low-energetic wave conditions in winter months remove sediments at the bottom of the beach in backrush and drop it during uprush, thus resulting in deposition (Joevivek and Chandrasekar, 2014). This implies that there is a strong connection between seasonal shoreline change and variations in wave actions. According to Awosika et al. (2013), beach ridge and barrier complexes along the Niger Delta coast are influenced by a combination of large swell and wind waves that approach the coast from the southwest, and by vigorous longshore drift generated by the waves. Also, wave-forcing of circulation in the surf zone is a major cause of sediment transport and shoreline morphology in all sectors of the ND (Awosika et al., 2013; Dada et al., 2016a, b). In the present study, a close connection between occurrences of peak wind speeds, wave heights and incidences of erosion is observed in the study area (Fig. 6 a-b). The critical incidences of negative shoreline changes as reported in this study also coincide with the occurrences of the highest peak wind speeds and wave heights (Figs 2-6). For instance, during the summer months, strong southwesterly winds of 4 m/s to 10 m/s are generated. This southwesterly monsoon wind produces high waves (1.5 and 3 m) and increasing periods (15-18 s) that could be related to the predominant erosion in summer months. With the end of the summer (mainly from May to October), the eroded shoreline is partly built up in the winter months (mainly from November to February). During the winter months, wind speed intensity fall to between 3 and 6 m/s. Likewise, wave heights and periods decrease to 0.8-1.6 m and 8-1.5 s, respectively (Fig. 5). The consequence of the intensity of the winds and waves conditions can be readily seen during this period (Fig. 2). Oyegun (1991) also noted at Forcados beach in the western ND that the magnitude and frequency of beach changes in Forcados are greater in the wet (summer months) season than in the dry (winter months) season. He further states that there was a net loss of beach materials in the wet season and a net gain in the dry season, even though erosion and accretion occurred throughout the year with no statistically significant difference in their magnitudes (Oyegun, 1991). Thus, one can infer that the reduction in the intensity of wind and wave conditions is responsible for shoreline advance observed in winter. Yates et al. (2011) and Osinowo et al. (2017) also confirm this by stating that the response of the beach to high-energy wave conditions is faster than to low-energy wave conditions.

Shoreline vulnerability to wave conditions depends on the difference between the wave frequency and shoreline recovery time, therefore wave effects can be accentuated if its frequency exceeds the shoreline recovery period. Likewise, when sand deposited seaward at a great water depth could not be brought back by the gentler winds and waves during calmer conditions, full shoreline recovery becomes impossible, thus resulting to negative shoreline change or recession in long-term (Harley et al., 2017; Kinsela et al., 2017). From this study, we find the foregoing to be true. For when shorelines are affected by prolonged or successive high energetic conditions and alternated with a short calm period, higher sediment volumes are lost and negative morphologic change is recorded. This is because recovery time in-between two extreme conditions is insufficient. For instance, the magnitude of erosion recorded during the summer months of 2011 and 2012 are higher than during the accretion in winter months of the same period (Fig. 2), which may result in deficit at the interannual scale. This corroborates the previous study on the evolution of the Niger Delta shoreline change by the Dada et al. (2015; 2016a, b; 2018). They reported that the entire ND shorelines retreated landwards over a period of 65 years (medium-term) and 90 years (long-term), however at short-term, it is presently prograding seaward (Dada et al., 2015).

Based on findings from this study, waves are gentler during the winter months because winds blow with less intensity and tend to deposit sands on the higher parts of the beach. Conversely, in the summer months, winds of greater intensity generate larger waves with more energy resulting from strong southwesterly offshore monsoonal winds, which activate cross-shore transports that are more persistent and tend to remove sediment from the upper parts of the beach and transport it offshore. This configuration tends to be reversed in another winter season, when accretion agents counter the forces of erosion, thereby resulting in a balance between erosion and deposition. These are the cases during all summer from 2009-2013 when erosions predominantly prevailed, and accretions during the subsequent period of calm conditions during the winter of 2010-2013 (Fig. 2). One can thus infer that a near-perfect periodic annual cycle of turbulence-fair weather cycle contributes to shoreline variations in the ND. That is, recession during the summer monsoon months and progradation during the winter months. However, most time shoreline is unable to recover all the sediment transported offshore during energetic period of the summer (rainy) months, because sediment is often lost to the canyons (Avon, Mahin and Calabar). As rightly expressed by Loureiro et al. (2011) and Quartel et al. (2008), seasonal cycle in shoreline change is driven by seasonality in wave forcing, especially in swell-dominated beaches like the study area.

4.1.2. THE RELATIONSHIP BETWEEN SHORELINE CHANGE AND THE HYDRODYNAMIC FORCING

To examine the dependence of the shoreline variations on the wind and wave forcing, the measured shorelines are correlated with the offshore wind and wave forcing. Figure 6 a-c shows the result of correlating shoreline variations with the average monthly offshore wind speeds and significant wave heights. A strong correlation of (0.903) exists between wind speed and the mean net shoreline change (Fig. 6a), implying a strong relationship between wind actions and shoreline in the study area. This relationship is stronger (0.962) in the case of wave height (Fig. 6b). Further, Figure 6 a-b vividly illustrates the relationships, trends and interactions that tend to occur between the hydrodynamics forcing of wind and wave and the shoreline during winter and summer in the study area. The first trend that occurs during summer shows that an increase in wind actions influences significant shoreline erosion (Fig. 6a). The second trend which occurs in winter indicates that when the wind actions decrease, the shoreline is increasingly accreted and prograded seaward (Fig. 6a). This is not different from the wave actions: an increase in the wave actions produces significant shoreline erosion, while its decrease results in accretion and seaward movement (Fig. 6b). The strong correlation that exists between the wind, wave forcing and the shoreline change demonstrates that winds and waves are key factors governing shoreline configuration in the study area. This result also shows that shoreline is in critical equilibrium with the energetic conditions. Analysis of wind and wave data from the area also shows a strong relationship between wind speed and wave height ($R^2 = 0.914$), as shown in Figure 6c.

Studies from other coasts around the world also reveal that seasonal changes in beach width are attributed to a seasonal variation in wave energy conditions with narrow beaches in winter and wide beaches in summer, e.g., Perth coastline, Australia (Masselink and Pattiaratchi, 2001) and

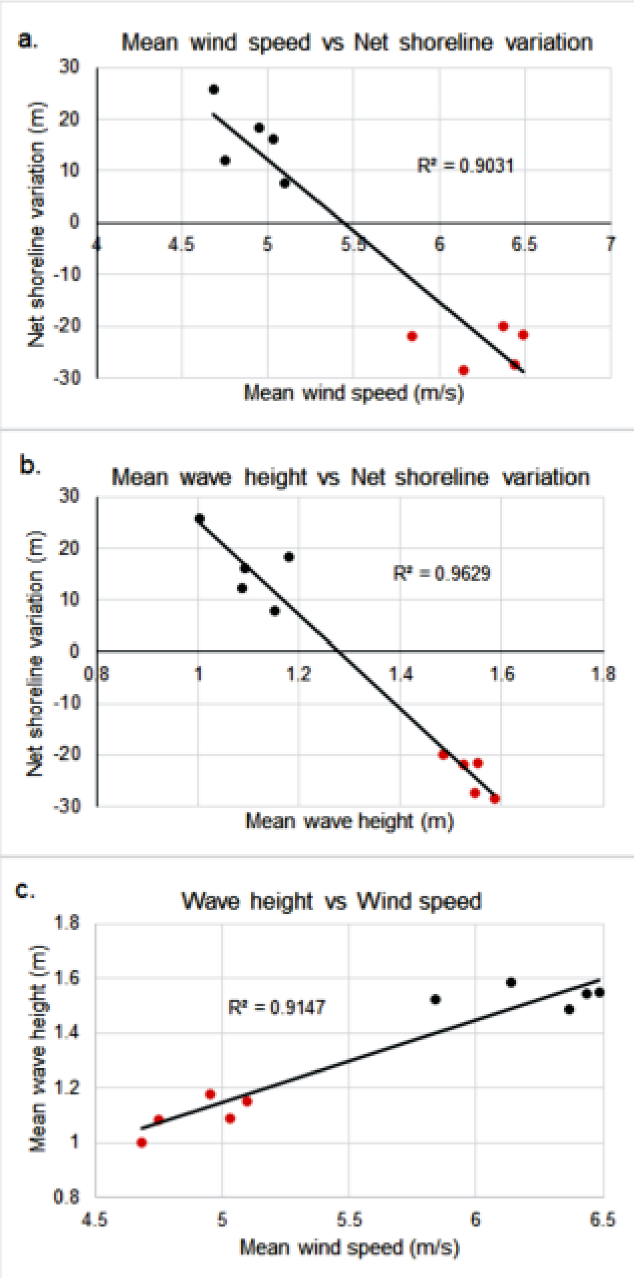

Figure 5. (a.) The correlation coefficient of seasonal shoreline variations with (a) wind condition and (b.) wave height shows a strong correlation (R^2=0.9031 and 0.9629, respectively). Figure 5 a-b could be considered as morphodynamic equilibrium curves with two trends. The first trend shows that an increase in the wind and/or wave energy level produces significant shoreline retreat, while the second trend indicates that, when the energy is low, the beach increasingly advance seaward. (c.) The correlation coefficient between mean wind speed and mean wave height is very strong (R^2=0.9147). These high correlations suggest strong influence that winds and waves have on shoreline configuration of the study area.

the coast of Maharastra, India (Bhat et al., 2003).

5. CONCLUSIONS

The present study investigated seasonal wind and wave climate and their implications on the Niger Delta (ND) shoreline variations in the Gulf of Guinea of the North Atlantic using shorelines from remote sensing data, coupled them with wind and wave data, for a period of 6 years (between 2008 and 2013). The following are the findings:

* Shoreline retreat occurs during the summer months of June to September (wet season), while a reversal (shoreline advance) occurs in the winter months of November to February (dry season).
* The southwesterly wind and waves predominate throughout the studied period, with long and high-energetic wind-induced wave conditions in summer months and low-energetic conditions during winter months.
* Strong correlations exist between the wind, wave forcing and the shoreline change, implying that these hydrodynamic forces influence shoreline configuration in the study area. Thus the shoreline indicates strong seasonal variability in erosion during summer months and accretion in winter months.
* This study contributes to the understanding of the environmental monitoring and protection, and coastal processes governing the Niger Delta coast.

REFERENCES

Abam, T.K.S., 2001. Regional hydrological research perspectives in the Niger Delta. Hydrological Sciences - Journal-des Sciences Hydrologiques, 46(1): 13-25.

Adejuwon, J.O., 2012. Rainfall seasonality in the Niger Delta Belt, Nigeria. J. Geogr. Reg. Plan. 5 (2): 51–60.

Accadia, C., Zecchetto, S., Lavagnini, A. and Speranza, A., 2007. Comparison of 10- m wind forecasts from a regional area model and QuikSCAT scatterometter wind observations over the Mediterranean Sea.Mon. Wea. Rev. 135: 1945–1960.

Alvarez, I., Gomez-Gesteira, M., deCastro, M. and Novoa, E. M., 2008. Ekman transport along the Galician Coast (NW, Spain) calculated from QuikSCAT winds. J. Mar. Syst. 72: 101–115.

Alvarez, I. and Coauthors, 2006. Use of MeteoGalicia wind data to monitor oil spills of the Galician coast: Comparison with QuikSCAT data.Cienc. Mar. 32(2B): 351– 360

Awosika, L.F, Folorunsho, R. and Imovbore, V., 2013. Morphodynamics and features of littoral cell circulation observed from sequential aerial photographs and Davies drifter along a section of the strand coast east of the Niger Delta, Nigeria. Journal of Oceanography and Marine Science, 4 (1): 12-18.

Bentamy, A., Ayina, H. L., Queffeulou, P., Croize-Fillon, D. and Kerbaol, V., 2007. Improved near real time surface wind resolution over the Mediterranean Sea.Ocean Sci. 3; 259–271.

Bhat, M.S., Chavadi, V.C., and Hegde, V.S., 2003. Morphology and sediment movement in a monsoon influenced open beach at Gangavali, near Gokarn (central west coast of India). Indian Journal of Marine Sciences, 32(1): 31-36.

Chelton, D. B., and Freilich, M. H., 2005. Scatterometter-based assessment of 10-m wind analyses from the operational ECMWF and NCEP numerical weather prediction models. Mon. Wea. Rev. 133: 409–429.

Cui, B.L. and Li, X.Y., 2011. Coastline change of the Yellow River estuary and its response to the sediment and runoff (1976-2005). Geomorphology: 127: 32–40.

Dada, O.A., Qiao, L.L., Ding, D., Li, G.X., Ma, Y.Y., Wang, L.M., 2015. Evolutionary trends of the Niger Delta Shoreline during the last 100 years: responses to rainfall and river discharge. Mar. Geol. 367: 202-211.

Dada, O.A., Li, G.X., Qiao, L.L., Ding, D., Ma, Y.Y., Xu, J.S., 2016a. Seasonal shoreline behaviours along the arcuate Niger Delta coast: complex interaction between fluvial and marine processes. Continental Shelf Res. 122: 51-67. https://doi.org/10.1016/j.csr.2016.03.002.

Dada, O.A., Li, G.X., Qiao, L.L., Ding, D., Ma, Y.Y., Xu, J.S., Li, P., Yang, J., 2016b. Response of wave and coastline evolution to global climate change off the Niger Delta during the past 110 years. Marine Systems 160: 64-80. https://doi.org/10.1016/j.marsys.2016.04.005.

Dada, O.A., Li, G.X., Qiao, L., Asiwaju-Bello, Y.A., Anifowose, A.Y.B., 2018. Recent Niger Delta shoreline response to Niger River hydrology: conflict between forces of nature and humans. J. African Earth Sciences 139: 222-231

Davidson, M.A., Lewis, R.P. and Turner, I.L.. 2010. Forecasting seasonal to multi-year shoreline change. Coastal Engineering 57 (6): 620-629.

Durduran, S.S., 2010. Coastline change assessment on water reservoirs located in the
Konya Basin Area, Turkey, using multi-temporal Landsat imagery. Environ Monit Assess 164:453–461.

Feng, Y.J., Liu, Y. and Liu, D., 2014. Shoreline mapping with cellular automata and the shoreline progradation analysis in Shanghai, China from 1979 to 2008. Arab J Geosci. https://doi.org/10.1007/s12517-014-1515-7.

Gokceoglu, C., Nefeslioglu, H.A., Turer, D., Akgun, A., Ayas, Z. and Temimhan, M., 2014. Determination of coastal border line: an integrated approach for a part of Antalya coast (Turkey). Arab J Geosci. https://doi.org/10.1007/s12517-014-1287-0

Harley, M.D., Turner, I.L., Kinsela, M.A., Middleton, J.H., Mumford,P.J., Splinter, K.D., Phillips, M.S., Simmons, J.A., Hanslow, D.J. and Short, A.D., 2017. Extreme coastal erosion enhanced by anomalous extratropical storm wave direction. Scientific Reports 7 (6033). DOI: 10 1038/s41598-017-05792-1

Hemer, M.A.; Church, J.A. and Hunter, J.R., 2007. Waves and climate change on the Australian coast, SI 50 (Proceedings of the 9th International Coastal Symposium), 432 – 437. Gold Coast, Australia.

Joevivek, V. and Chandrasekar, N., 2014. Seasonal impact on beach morphology and the status of heavy mineral deposition-central Tamil Nadu coast, India. J. Earth Syst. Sci. 123 (1):135–149.

Kinsela, M. A., Morris, B. D., Linklater, M. & Hanslow, D. J., 2017. Second-Pass Assessment of Potential Exposure to Shoreline Change in New South Wales, Australia, Using a Sediment Compartments Framework. J. Mar. Sci .& Eng. 6 1 (4) . https://doi.org/10.3390/jmse5040061

Kuenzer, C., van Beijma, S., Gessner, U., Dech, S., 2014. Land surface dynamics and environmental challenges of the Niger Delta, Africa: remote sensing-based analyses spanning three decades (1986–2013). Appl. Geogr. 53: 354–368.

Louati, M., Saïdi, H. and Zargouni, F., 2014. Shoreline change assessment using remote sensing and GIS techniques: a case study of the Medjerda delta coast, Tunisia. Arab J Geosci. https://doi.org/10.1007/s12517-014-1472-1.

Loureiro, C., Ferreira, O., and Cooper, J.A.G., 2011. Morphologic change and morphodynamic at high-energy embayed beaches in Southwestern Portugal. In proceeding of: Coastal Sediments '2011: 2:1375-1389. https://doi.org/10.1142/8190

Masselink, G., Pattiaratchi, C.B., 2001. Seasonal changes in beach morphology along the sheltered coastline of Perth, Western Australia. Mar Geol 172:243–263.

Olaniyan, E. and Afiesimama, E. A., 2003.

Understanding ocean surges and possible signals over the Nigerian coast: a case study of the Victoria Island Bar-Beach Lagos.http://iodeweb1.vliz.be/odin/bitstream/1834/420/1/Aniola_Nigeria.pdf (accessed May 2, 2018).

Osinowo, A.A., Okogbue, E.C., Eresanya, E.O. and Akande, O.S., 2017. Evaluation of wind potential and its trends in the mid-Atlantic, 2017. Modeling Earth Systems and Environment 3 (4):1199–1213.

Oyegun, C.U., 1991. Spatial and seasonal aspects of shoreline changes at Forcados Beach, Nigeria. Earth Surface Processes and Landforms, 16(4):293-305.

Penabad, E., Alvarez, I., Balseiro, C. F., deCastro, M., Go´mez, B., Pe´rez-Mun ˜uzuri, V. and Go´mez-Gesteira, M., 2008. Comparative analysis between operational weather prediction models and QuikSCAT wind data near the Galician coast.J. Mar. Syst. 72: 256–270.

Pensieri, S., Bozzano, R. and Schiano, M. E., 2010. Comparison between QuikSCAT and buoy wind data in the Ligurian Sea. J. Mar. Syst. 81: 286–296.

Pianca, C., Mazzini, P.L.F. and Siegle, E., 2010. Brazilian offshore wave climate based on NWW3 reanalysis. Brazilian Journal of Oceanography, 58(1):53-70

Pickett, M. H., Tang, W., Rosenfeld, L. K. and C. H. Wash, 2003. QuikSCAT satellite comparisons with nearshore buoy wind data off the U.S. west coast.J. Atmos. Oceanic Technol. 20: 1869–1879.

Quartel, S, Kroon, A and Ruessink, B.G., 2008. Seasonal accretion and erosion patterns of a microtidal sandy beach. Marine Geology, 250 (1–2): 19–33.

Rusu, L., Pilar, P., Guedes-Soares, C., 2008. Hind-cast of the wave conditions along the west Iberian coast. Coastal Engineering, 55 (11):906-919.

Ruti, P. M., Marullo, S., D'Ortensio, F. and Tremant, M., 2008. Comparison of analyzed and measured wind speeds in the perspective of oceanic simulations over the Mediterranean basin: Analyses, QuickSCAT, and buoy data. J. Mar. Sci. 70: 33–48.

Satheesan, K., Sarkar, A., Parekh, A., Ramesh Kumar, M. R. and Kuroda, Y., 2007. Comparison of wind data from QuikSCAT and buoys in the Indian Ocean.Int. J. Remote Sens. 10: 2375–2382.

Sebastião, P., Guedes-Soares, C., Booij, N., 2000. Wave hind-casting off the coast of Portugal. Coastal Engineering, 40 (4),411-425.

Splinter, K.D., Davidson, M.A., Golshani, A., Tomlinson, R., 2012. Climate controls on longshore sediment transport. Continental Shelf Research 48:146–156.

Tang, W., Liu, W. T. and Stiles, B. W., 2004. Evaluation of highresolution ocean surface vector winds measured by QuikSCAT scatterometer in coastal regions. IEEE Trans. Geosci. Remote Sens. 42: 1762–1769.

Thieler, E.R., Smith, T.L., Knisel, J.M., and Sampson, D.W., 2013. Massachusetts Shoreline Change Mapping and Analysis Project, 2013 Update: U.S. Geological Survey Open-File Report 2012-1189, 42 p. http://pubs.usgs.gov/of/2012/1189/.

Thieler, E.R., Himmelstoss, E.A., Zichichi, J.L., and Ergul, Ayhan, 2009. Digital Shoreline Analysis System (DSAS) version 4.0- An ArcGIS extension for calculating shoreline change: U.S. Geological Survey Open-File Report 2008- 1278. *Version 4.3.

Wallcraft, A.J., Kara, A. B., Barron, C. N., Metzger, E. J., Pauley, R. L. and Bourassa, M. A., 2009. Comparisons of monthly mean 10 m wind speeds from satellites and NWP products over the global ocean. Journal of Geophysical Research 114: D16109.

Yates, M. L., R. T. Guza, W. C. O'Reilly, J. E. Hansen, and P. L. Barnard, 2011. Equilibrium shoreline response of a high wave energy beach, J. Geophys. Res., 116, C04014, https://doi.org/10.1029/2010JC006681.